Analytical mechanics of asteroid disassembly using the Orbital Siphon effect

Andrea Viale[a*]
a.viale.1@research.gla.ac.uk

Colin McInnes[b]
Colin.Mcinnes@glasgow.ac.uk

Matteo Ceriotti[c]
Matteo.Ceriotti@glasgow.ac.uk

a,b,c: University of Glasgow, Glasgow G12 8QQ, UK.
* : corresponding author.

Abstract

A chain of tether-connected payload masses assembled from the surface material of a spherical rotating asteroid is envisaged as a means of delivering a fraction of the asteroid mass into orbit, without the need of external work to be done. Under conditions to be discussed, a net radial force is established on the chain which can be exploited to initialize an *orbital siphon* effect: new payloads are connected to the chain while top payloads are removed and released into orbit. Adopting simplifying assumptions, the underlying dynamics of the problem is entirely analytical and is investigated in detail. The amount of mass extractable from the asteroid is then discussed, according to a range of strategies. It is proposed that the scheme could in future provide an efficient means of extracting material resources from rotating Near Earth Asteroids.

1 Introduction

Exploitation of the resources available in space is one of the key challenges for future space exploration. Many of these resources have been recognized as potentially low-cost alternatives to those launched from Earth. In particular, Near Earth Asteroids are among the easiest objects to reach and could provide resources such as water, liquid propellants, semiconductors, and metals [1]. Several studies, such as [2], have shown that a useful mass of accessible resources may be available to be transferred into Earth orbit with transfer energies lower than that required to exploit the Moon (which is less abundant in some useful materials with respect to asteroids [3]). To address this problem, different scenarios can be envisaged to transfer material to Earth-orbit, such as transport of the entire asteroid or transport of mined material, the optimal choice depending on the particular asteroid of interest.

A further possibility is in-situ manufacturing using asteroid resources, for example to assemble space-structures directly nearby the asteroid or process water for propellants or life support. In the latter case, asteroid partial disassembly may be useful to harvest water using solar concentrator technologies [4].

Motivated by this growing interest in asteroid resource exploitation, this paper investigates a new strategy to deliver a fraction of the asteroid mass into orbit or

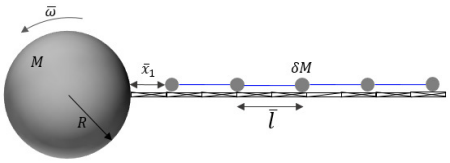

Figure 1: Model for the chain of masses.

to escape. The analysis has its roots in the idea of leveraging the rotational kinetic energy of a rotating body to overcome its gravity, firstly developed by Tsiolovski [5, 6] then improved by Artsutanov [7] and Pearson [8, 9] with the concept of space elevator. The elevator is envisaged as a tethered structure to connect a mass in synchronous (or higher) orbit and the surface of the body. The tether is in equilibrium by the balance of centripetal and gravitational forces acting on it; the payload is then lifted to the desired altitude along the tether and, if synchronous orbit is reached, the payload could increase its altitude without further work required. A wide range of studies are available in the literature, investigating design, materials, tether oscillation and stability [10, 11, 12, 13, 14, 15, 16, 17], mainly for Earth applications.

A direct evolution of the space elevator is the *orbital siphon* concept firstly introduced by Davis and elaborated by McInnes [18], which is the foundation of this work. In this case, rather than a single payload ascending along the tether, a chain of connected masses is envisaged, where the centripetal pull due to the body's spin can overcome the gravitational force on the payloads, eventually allowing payloads to escape. Longsdon [19] pictured an equivalent concept for fluids, where a pipeline is used instead of a chain of masses, to raise sea water above syncronous Earth orbit. Speculatively, he has shown that the water flux may drive turbines to generate power.

A chain of payloads (*siphon effect*) can therefore be envisaged to provide a continuous mass flow from the surface of the rotating asteroid into orbit: new payloads are connected to the chain while top payloads are removed and released into orbit, without the need for external work to be done. Under some assumptions, this paper shows that an analytical approach can be developed for a vertical chain of payload masses, taking into account the angular velocity decrease of the asteroid due to mass removal and the consequent decrease in centripetal-induced lift force. Different strategies of mass extraction are taken into account considering fixed-length and variable-length chains; for each of them, the maximum amount of extractable material is determined. Dynamical time-scales and mass flow rates are also considered.

The paper is organized as follows. Section 2 introduces the model of the orbital siphon. Conservation of angular and linear momentum are applied to study the evolution of the angular velocity of the asteroid as it undergoes mass loss (Sect.22.1) and the radial velocity of the chain (Sect.22.2) respectively. The specific energy of the released material as a function of relevant parameters is then studied (Sect.22.3).

Section 3 analyses siphon operation. Possible extraction scenarios are then described in Sects. 33.1 (chain of masses with constant length) and 3.2 (chain of masses with variable length). Discussions and conclusions follow in Sects. 4 and 5.

2 System description

The model consists of a spherical asteroid with radius R, mass M rotating as a rigid body with angular velocity $\bar{\omega}$. A total of $n \geq 2$ payload masses (PMs) can slide frictionless along a rigid truss fixed at a point along the equator of the asteroid, as shown in Fig. 1. The truss supports the transversal Coriolis force due to the radial

motion of the chain. Each PM is connected to the neighbouring masses by a (massless) tether with length $\bar{l}$ and infinite stiffness. The total length of the chain is therefore $\bar{L} = (n-1)\bar{l}$. The following assumptions are made:

1. Each PM is considered a point-like mass δM, such that $\delta M/M << 1$.
2. The gravitational interaction between PMs is neglected. The sole gravitational interaction is between each PM and the asteroid.
3. The density ρ of the asteroid is constant and uniform.
4. The effects of the asteroid's orbit on the dynamics are neglected.
5. The truss is infinitely rigid, i.e., its deformations and interactions with the chain are neglected.
6. No external forces are acting on the asteroid and chain.
7. The centre of mass of the coupled system asteroid and chain is assumed to be coincident with the centre of mass of the asteroid.

As a consequence of these assumptions, the system has only one degree of freedom, i.e., the altitude $\bar{x}_1$ of the first PM.

Within a reference frame rotating with the asteroid, each PM is subjected to gravitational and centripetal forces, as well as the internal tensions along the tether. It is assumed that the i-th tether connects the i-th and the $(i+1)$-th PM. Note that the transversal Coriolis force does not interfere with the radial motion of the chain if friction is neglected. The overall force on the i-th PM is the sum of the gravitational and centripetal force and the tether tensions. This can be expressed as:

$$\bar{f}_i = -G\frac{M\delta M}{\left(R+\bar{x}_i\right)^2} + \delta M\bar{\omega}^2\left(R+\bar{x}_i\right) + \bar{N}_i - \bar{N}_{i-1}, \quad i = 1,\ldots,n \tag{1}$$

where $G = 6.674 \times 10^{-11}\,\mathrm{m^3 kg^{-1} s^{-2}}$ is the gravitational constant, $\bar{x}_i = \bar{x}_1 + (i-1)\bar{l}$ is the altitude of the i-th mass and $\bar{T}_i$ is the tension on the i-th tether, connecting the i-th and the $(i+1)$-th PM (the total number of tethers is therefore $n-1$). The variable $\bar{x}$ (without subscript) will also be used in this section to indicate the altitude of a generic point along the chain. Equation (1) can be rewritten in non-dimensional form as

$$f_i = -\frac{1}{\left[1+\chi+(i-1)l\right]^2} + \omega^2\left[1+\chi+(i-1)l\right] + N_i - N_{i-1} \tag{2}$$

where

$$f_i = \frac{\bar{f}_i}{GM\delta M/R^2} \tag{3a}$$

$$N_i = \frac{\bar{N}_i}{GM\delta M/R^2} \tag{3b}$$

and

$$l = \frac{\bar{l}}{R}, \quad \chi = \frac{\bar{x}_1}{R} \tag{4}$$

$$\omega = \frac{\bar{\omega}}{\bar{\omega}_{crit}}, \quad \bar{\omega}_{crit} = \sqrt{\frac{\mu}{R^3}} = 2\sqrt{\frac{G\rho\pi}{3}} \tag{5}$$

with $\mu = GM$. Then, $\bar{\omega}_{crit}$ is the critical angular velocity of the asteroid. When $\bar{\omega} = \bar{\omega}_{crit}$ the gravitational force on a particle δM at the equator of the asteroid is equal (in absolute value) to the centripetal force. In this paper it is assumed $\omega \in [0,1]$. Note that the parameter ω contains information about both the angular velocity of the asteroid and its density. The overall force on the whole chain is then $f = \sum_{i=1}^{n} f_i$.

Performing the summation the internal tensions T_i vanish and the net resultant force on the chain of masses is given by (see also [18])

$$f = \frac{1}{l^2}\left[\Psi^{(1)}\left(\frac{1+nl+\chi}{l}\right) - \Psi^{(1)}\left(\frac{1+\chi}{l}\right)\right] + \omega^2 n\left(1 - \frac{l}{2} + \chi + \frac{nl}{2}\right) \tag{6}$$

where $\Psi^{(m)}(z)$ is the polygamma function of order m [20], defined in series as

$$\Psi^{(m)}(z) = (-1)^{m+1} m! \sum_{i=0}^{\infty} (z+i)^{-(m+1)}. \tag{7}$$

Form the definition (4) it follows that the product $\lambda = nl$ appearing in Eq. (6) is related to the normalized length of the chain $L = \bar{L}/R$. In fact:

$$\lambda = nl = n\frac{\bar{l}}{R} = \frac{(n-1)\bar{l}}{R} + \frac{\bar{l}}{R} = L + l. \tag{8}$$

It can be shown that $\frac{df}{d\chi} > 0$ for every $l > 0$, n and $\omega \in [0, 1]$. Hence the overall force increases with an increase of the altitude χ of the first mass. The motion of the chain is described by

$$n\delta M \frac{d^2}{dt^2}\bar{x}_1 = \sum_{i=1}^{n} \bar{f}_i. \tag{9}$$

Using Eqs. (2),(4), (5) and (6), Eq. (9) can be written in non-dimensional form as

$$\ddot{\chi} = \frac{f}{n\omega^2} \tag{10}$$

where $\ddot{\chi}$ represents the non-dimensional acceleration of the first PM

$$\ddot{\chi} = \frac{1}{\bar{\omega}^2 R}\frac{d^2}{dt^2}\bar{x}_1. \tag{11}$$

Similarly, $\dot{\chi}$ is defined as

$$\dot{\chi} = \frac{1}{\bar{\omega} R}\frac{d}{dt}\bar{x}_1. \tag{12}$$

For a given χ, if $f = 0$ the chain will be in equilibrium. Following the analysis in [18] it can be shown that the equilibrium is unstable.

The normalized tensions T_i can be calculated solving the system of equations (2) once the chain acceleration $\ddot{\chi}$ is known from Eq. (9) (clearly, if the chain is in equilibrium $\ddot{\chi} = 0$). Figure 2 shows the normalized tension along the tethers at equilibrium ($f = 0$) with $\chi = 0$ for three values of ω and $n = 25$ (a), $n = 50$ (b), with respect to the normalized altitude $x = \bar{x}/R$. Note that the chain length L varies for the angular velocities chosen, according to Eq. (6) with $f = 0$ and Eq. (8). The maximum tension is reached for the tether crossing the synchronous orbit altitude $\bar{x}_{sync}$, which can be expressed as a function of ω from the definition of synchronous orbit altitude

$$\frac{2\pi}{\sqrt{\mu}}(R + \bar{x}_{sync})^{3/2} = \frac{2\pi}{\bar{\omega}} \tag{13}$$

and using the definition of $\bar{\omega}_{crit}$ (Eq. (5)), to obtain:

$$x_{sync} = \frac{\bar{x}_{sync}}{R} = \omega^{-2/3} - 1. \tag{14}$$

The non-dimensional synchronous orbit altitude x_{sync} is indicated with a dotted line in Fig. 2 for each ω considered. For a given ω the maximum tension becomes larger as the number of PMs is increased while, for a given n, smaller tensions are found as ω approaches the critical angular velocity.

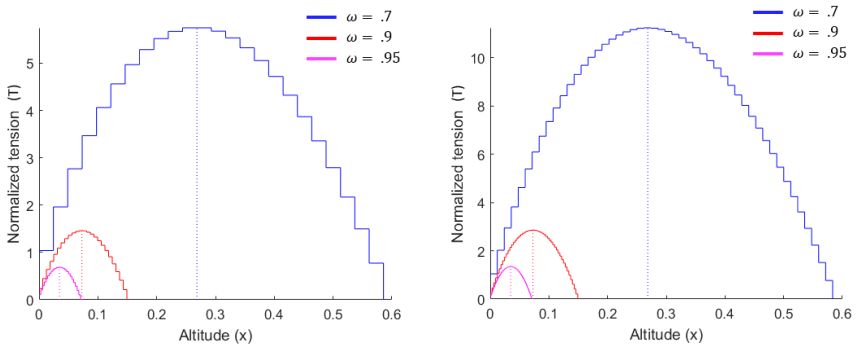

(a) (b)

Figure 2: Normalized tension along the tethers for $n = 25$ (a) and $n = 50$ (b) at the equilibrium ($f = 0$). The dotted lines represent the syncronous orbit altitude for the given ω. (Online version in colour).

For any $k > 0$ the polygamma function $\Psi^{(1)}$ has the following property:

$$\lim_{z \to +\infty} x\Psi^{(1)}(kz) = \frac{1}{k}. \tag{15}$$

Equation (15) can then be used to rearrange Eq. (6) when the chain length L is fixed and the number of PMs becomes large. In this case $n \to \infty$ with $l \to 0$ and, from Eq. (8), $\lambda \to L$, i.e., λ approaches the ratio between the length of the chain and the asteroid radius. Upon simplification, Eq. (6) becomes

$$f^* = -\frac{n}{1+\lambda} + \omega^2 n \left(1 + \frac{\lambda}{2}\right). \tag{16}$$

Then, it follows from Eq. (16) that the normalized chain length λ_{eq} that guarantees equilibrium of the chain ($f^* = 0$) depends only on ω. In particular, solving Eq. (16) for $f^* = 0$ with respect to λ and considering the positive solution yields:

$$\lambda_{\text{eq}} = \frac{1}{2}\left[\sqrt{9 - 8\left(1 - \frac{1}{\omega^2}\right)} - 3\right]. \tag{17}$$

If Eq. (17) is specialized in the case of the Earth ($\omega \approx 0.058$) then the equilibrium length is the same as the limit found by [8] for a continuous hanging tower. Clearly, λ_{eq} decreases as the angular velocity of the asteroid approaches the critical angular velocity (eventually it vanishes for $\omega = 1$), while it tends to infinity as ω tends to zero.

Figure 3 shows the relative error between Eq. (16) and Eq. (6) to evaluate the chain length λ at equilibrium, as a function of n and for three values of ω. The solution to $f^* = 0$ clearly approaches λ_{eq} as n becomes larger. The relative error is below 3% for $\omega > 0.5$ and $n \geq 50$: under such conditions Eq. (17) can be regarded as a good approximation to the solution of $f = 0$. Moreover, the equilibrium length calculated with Eq. (6) is always larger than λ_{eq}, i.e., for a given ω, the equilibrium length of a chain with finite n is always larger than the equilibrium length of a chain with $n \to \infty$. Therefore, if $f^* = 0$ for a given ω and λ, then $f > 0$ for any n.

If $f > 0$ (or $f^* > 0$ for large n) then an orbital siphon effect can be envisaged, where a new payload is attached to the chain and simultaneously the top one is removed. To asses this scenario, conservation principles are applied to model the dynamics. In particular, conservation of angular momentum (Sect. 2.1) allows the variation of

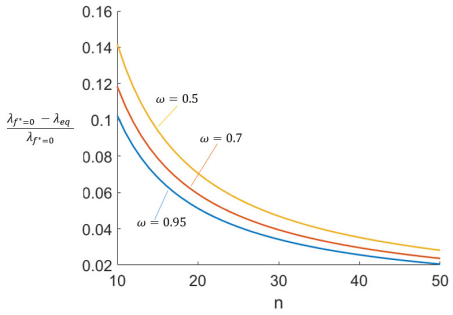

Figure 3: Relative error when using Eq. (16) in place of Eq. (6) to find the equilibrium length of the chain.

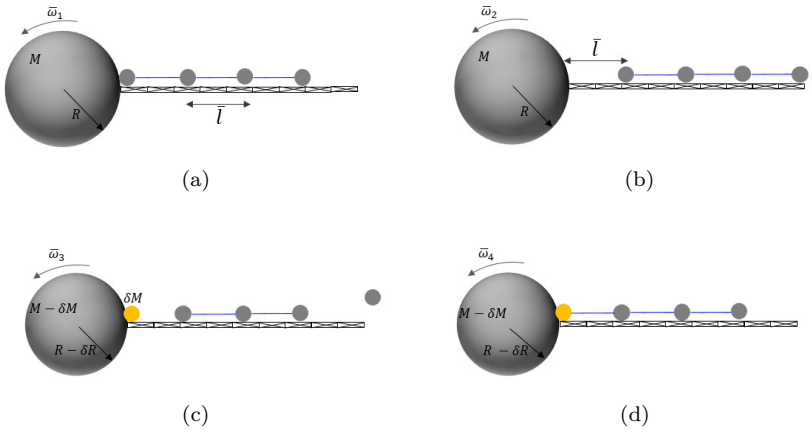

Figure 4: Four-step sequence to model the extraction of a payload mass. In this case a chain with $n = 4$ is represented.

the angular velocity of the asteroid and chain to be investigated as a consequence of mass extraction, while conservation of linear momentum together with the kinetic energy theorem (Sect. 2.2) allows the evolution of the chain velocity to be investigated. Conservation of mass is applied to model the mass decrease of the asteroid. Note that the actual mining techniques used to extract mass from the asteroid are beyond the scope of this paper.

2.1 Conservation of angular momentum

The extraction of a PM from the asteroid and the subsequent release of the top PM from the chain is modelled through a four-step sequence (see Fig. 4):

1. Initially the bottom PM is on the surface, $\chi = 0$ (Fig. 4a) and, in general, $\dot{\chi} \geq 0$. If $f > 0$ the chain will lift.
2. The chain has lifted by $\chi = l$ (Fig. 4b).
3. The top PM is released and a new mass δM is positioned at the surface of the asteroid. Consequently, the asteroid mass decreases by δM to guarantee conservation of mass (Fig. 4c).

4. The bottom PM is connected to the chain (Fig. 4d) so that the chain is in the same geometrical configuration as step 1, with $\chi = 0$.

This sequence is then repeated, with the chain constantly operating with $\chi \in [0, l]$. A set of steps from 1 to 4 defines an iteration. Let R_j, M_j, $I_{A,j}$ and $\bar{\omega}_j$ be the radius, mass, inertia and angular velocity of the asteroid at the j-th step ($j = 1, \ldots, 4$) of the k-th iteration (to avoid confusion in notation, the reference to the k-th iteration is omitted at this stage). Similarly, $I_{C,j}$, χ_j and $\dot{\chi}_j$ are the moment of inertia and position and velocity of the chain. It follows:

$$I_{A,j} = \frac{2}{5} M_i R_i^2, \qquad j = 1, 2, 3, 4 \tag{18a}$$

$$I_{C,j} = \delta M R_j^2 \sum_{i=1}^{b_j} (1 + \chi_i + (i-1)l)^2, \qquad j = 1, 2, 3, 4 \tag{18b}$$

where

$$b_1 = n, \quad b_2 = n, \quad b_3 = n - 1, \quad b_4 = n \tag{19}$$

and

$$\chi_1 = 0, \quad \chi_2 = l, \quad \chi_3 = l, \quad \chi_4 = 0. \tag{20}$$

The mass of the asteroid changes at step 3. As conservation of mass holds, it is assumed that the sphere loses its outer shell of mass δM and thickness δR to form the new PM which is then positioned on the surface of the asteroid (although, in practice, the change in shape of the asteroid due to mass extraction would depend on the process used to gather mass at the base of the siphon). Hence:

$$\begin{array}{llll} M_1 = M, & M_2 = M, & M_3 = M - \delta M, & M_4 = M - \delta M, \\ R_1 = R, & R_2 = R, & R_3 = R - \delta R, & R_4 = R - \delta R. \end{array} \tag{21}$$

Note that $M = 4/3\pi R^3 \rho$ and, by differentiation, $\delta M = 4\pi R^2 \rho \delta R$. Therefore:

$$\frac{\delta R}{R} = \frac{1}{3} \frac{\delta M}{M}. \tag{22}$$

As no external torques are acting on the asteroid and chain, conservation of angular momentum holds at each step. Therefore:

$$(I_{A,j} + I_{C,j})\bar{\omega}_j = (I_{A,j+1} + I_{C,j+1})\bar{\omega}_{j+1}, \qquad j = 1, 2, 3. \tag{23}$$

Substituting Eqs. (18) and (22) into Eq. (23) and simplifying yields:

$$\frac{\delta\bar{\omega}_{12}}{\bar{\omega}_1} = 5\left(\lambda + \frac{1}{2}\lambda^2\right)\frac{\delta M}{M} + \text{h.o.t.} \tag{24a}$$

$$\frac{\delta\bar{\omega}_{23}}{\bar{\omega}_2} = \frac{5}{6}\frac{\delta M}{M} + \text{h.o.t.} \tag{24b}$$

$$\frac{\delta\bar{\omega}_{34}}{\bar{\omega}_3} = 0 \tag{24c}$$

where $\delta\bar{\omega}_{12} = \bar{\omega}_2 - \bar{\omega}_1$, $\delta\bar{\omega}_{23} = \bar{\omega}_3 - \bar{\omega}_2$, $\delta\bar{\omega}_{34} = \bar{\omega}_4 - \bar{\omega}_3$ and the higher order terms (h.o.t.) are neglected. Therefore:

$$\frac{\delta\bar{\omega}_{23}}{\bar{\omega}_2} = \frac{\delta\bar{\omega}_{23}}{\bar{\omega}_1 - \delta\bar{\omega}_{12}} = \frac{\delta\bar{\omega}_{23}}{\bar{\omega}_1}\left(1 + \frac{\delta\bar{\omega}_{12}}{\bar{\omega}_1}\right) + \text{h.o.t.} = \frac{\delta\bar{\omega}_{23}}{\bar{\omega}_1} + \text{h.o.t.}. \tag{25}$$

Equivalently, it can be shown that

$$\frac{\delta\bar{\omega}_{34}}{\bar{\omega}_3} = \frac{\delta\bar{\omega}_{34}}{\bar{\omega}_1} + \text{h.o.t.} \tag{26}$$

Hence, by neglecting again the h.o.t., Eqs. (24) can be summed to find the overall angular velocity variation $\delta\bar{\omega} = \delta\bar{\omega}_{12} + \delta\bar{\omega}_{23} + \delta\bar{\omega}_{34}$ between step 1 and 4:

$$\frac{\delta\bar{\omega}}{\bar{\omega}} = 5\left(\frac{1}{6} + \lambda + \frac{1}{2}\lambda^2\right)\frac{\delta M}{M}, \tag{27}$$

where the subscript 1 has been removed from $\bar{\omega}$ for clarity. Equation (27) dictates that the overall variation of angular velocity from step 1 to 4 is proportional to the ratio $\delta M/M$ through a coefficient depending only on λ.

From hypothesis 3 in Sect. 2 and the definition of the critical angular velocity $\bar{\omega}_{crit}$ (Eq. (5)) it follows immediately that $\bar{\omega}_{crit}$ does not change between steps 1 and 4; therefore

$$\frac{\delta\bar{\omega}}{\bar{\omega}} = \frac{\delta\bar{\omega}/\bar{\omega}_c}{\bar{\omega}/\bar{\omega}_c} = \frac{\delta\omega}{\omega}. \tag{28}$$

This identity will be useful in later analysis.

2.2 Chain radial velocity

The radial velocity of the chain is described by the non-dimensional parameter $\dot{\chi}$. If $f > 0$ the chain will rise between step 1 and 2. The non-dimensional work $W(\chi)$ done by the force f to raise the chain from 0 to $\chi \in [0, l]$ can be written as:

$$W(\chi) = \int_0^{\chi} \ddot{\chi} d\chi \tag{29}$$

where the acceleration $\ddot{\chi}$ is given by Eq. (10). Note that the non-dimensional work $W(\chi)$ is related to the dimensional work $\bar{W}(x_0)$ through $W(\chi) = \bar{W}(x_0)/(\delta M\bar{\omega}^2 R^2)$. From the kinetic energy theorem:

$$W(\chi) = \frac{\dot{\chi}^2}{2} - \frac{\dot{\chi}_1^2}{2}. \tag{30}$$

where $\dot{\chi}_1$ is the non-dimensional velocity of the chain for $\dot{\chi} = 0$. Hence, the velocity of the chain as a function of the position χ can be written as

$$\dot{\chi} = \sqrt{\dot{\chi}_1^2 + 2W(\chi)}. \tag{31}$$

In particular, at step 2, $\chi = \chi_2 = l$. In this case $W(l)$ can be evaluated analytically:

$$W(l) = \frac{l}{2}\left(2 + nl - \frac{2}{(1+nl)\omega^2}\right). \tag{32}$$

Then, equation (31) simply becomes:

$$\dot{\chi_2} = \sqrt{\dot{\chi}_1^2 + 2W(l)}. \tag{33}$$

At step 3 the top PM is released from the chain. In the inertial frame there are no external forces acting on the asteroid and chain (assumption 6), hence conservation of linear momentum holds. Conserving linear momentum between step 2 and 3 yields [1]:

$$\dot{\chi}_3 = \dot{\chi}_2. \tag{34}$$

Therefore the release of the top mass does not alter the radial velocity of the chain.

[1] The proof to Eqs. (34) and (35) is omitted due to constraints in page limit. It involves simple algebraic manipulation, considering the velocities of the PMs in the inertial frame.

At step 4 the bottom PM, which is initially at rest, is connected to the asteroid. Again, applying conservation of linear momentum between steps 3 and 4 yields:

$$\dot{\chi}_4 = \frac{n-1}{n}\dot{\chi}_3. \tag{35}$$

The sequence is then repeated from step one, with a new $\dot{\chi_1}$ equal to the last PM velocity $\dot{\chi_4}$.

Now, let $\dot{\chi_3}^k$ be the value of the radial release velocity $\dot{\chi_3}$ at the k-th iteration. Then, it follows from Eqs. (33), (34) and (35) that

$$\dot{\chi_3}^k = \sqrt{\left(\frac{n-1}{n}\right)^2 \left(\dot{\chi_3}^{k-1}\right)^2 + 2W(l)} \tag{36}$$

It can be shown that the recursive sequence $\left\{\dot{\chi_3}^k\right\}$ is bound and monotonic and hence converges. Let v_l be the limit of the sequence. Its value can be found noting that $v_l = \lim_{k\to\infty} \dot{\chi_3}^k = \lim_{k\to\infty} \dot{\chi_3}^{k-1}$. Then $v_l = \sqrt{\left(\frac{n-1}{n}\right)^2 v_l^2 + 2W(l)}$, hence

$$v_l = \sqrt{\frac{2W(l)}{1-\left(\frac{n-1}{n}\right)^2}} \tag{37}$$

which represents the normalized radial release velocity of the chain at steady state. The velocity v_l depends on the length of the chain and the normalized angular velocity of the asteroid. Clearly, ω will change during the transient due to mass extraction (Eq. (27)) but, as the steady state is approached within a few iterations, this variation can reasonably be neglected.

Note that v_l is a finite value. Hence, even though the chain is subjected to a non-zero force, its velocity does not diverge. In fact, although the chain does accelerate between step 1 and 2, its velocity then decreases at step 4, as a new PM is attached to the chain, in order to conserve linear momentum. As the tethers are assumed to be rigid, the change in velocity is instantaneous. At the end of the section this rigid-chain model is compared with an elastic chain model.

Note that $v_l > 0$ for $W(l) > 0$. By analysis of Eq. (32) it is straightforward to show that $W(l) > 0$ if $\lambda > \lambda_{eq}$. It has been noted in Sect. 2 that if $f = 0$ then $\lambda > \lambda_{eq}$. Therefore, even if the force on the chain is initially zero at the first iteration, any arbitrary small perturbation such that $\dot{\chi}_1 > 0$ will initialize the lifting process, and the release velocity at steady state will be positive as dictated by Eq. (37).

It is interesting to evaluate Eq. (37) when the number of masses on the chain becomes large. This can be done calculating the limit of Eq. (37) for $n \to \infty$:

$$v_l^* = \lim_{n\to\infty} v_l = \sqrt{\frac{\lambda}{2}\left(2 + \lambda - \frac{2}{(1+\lambda)\omega^2}\right)}. \tag{38}$$

When using Eq. (38) as an approximation of Eq. (37) for the radial velocity of a PM at release, the relative error is a function of n only:

$$\left|\frac{v_l - v_l^*}{v_l}\right| = 1 - \frac{\sqrt{2}}{2}\sqrt{2 - \frac{1}{n}}. \tag{39}$$

This error is lower than 1% for $n > 25$. Therefore, Eq. (38) is an accurate approximation of the radial release velocity (37) and is a sole function of the normalized length of the chain and the normalized angular velocity of the asteroid.

Equation (31) can be used to find the time P required for the chain to rise from $\chi = 0$ to $\chi = l$. In fact, noting $\tau = \bar{\omega}t$ then from Eq. (12) $\dot{\chi} = d\chi/d\tau$. It follows:

$$d\tau = \frac{d\chi}{\sqrt{\dot{\chi}_1^2 + 2W(\chi)}} \tag{40}$$

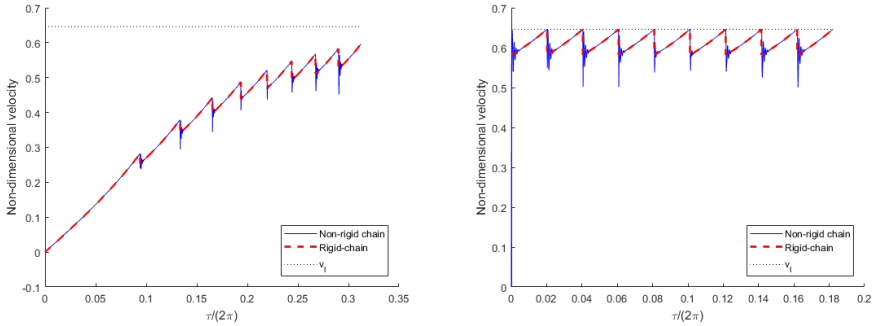

(a) (b)

Figure 5: Rigid chain model and flexible chain model velocity compared during transient (a) and at steady state (b).

where $W(\chi)$ is evaluated from Eq. (29). At steady state, $\dot{\chi}_1 = \frac{n-1}{n} v_l$. Then the time P to raise a PM becomes

$$P = \int_0^l \frac{1}{\sqrt{\left(\frac{n-1}{n}\right)^2 v_l^2 + 2W(\chi)}} d\chi. \tag{41}$$

Note that P is non-dimensional and a unit of rotation is defined by $P = 2\pi$. The ratio $N = \frac{2\pi}{P}$ therefore represents the number of released PMs per rotational period of the asteroid and it will be used in later analysis.

By removing the hypotheses of tethers with infinite stiffness, the resulting system with n degrees of freedom (DOF) will oscillate every time a new PM is added to the chain. In fact the first PM, with initial zero radial velocity, is pulled by the other PMs of the chain characterized by non-zero radial velocity, thus producing a tension in the lowermost tether which is then propagated along the chain. Figure 5 shows the difference between the rigid chain model used in this section and a n-DOF model where the PMs are linked via tethers with rigidity k and damping c. The problem can be described using the additional non-dimensional parameters $\frac{\sqrt{k/\delta M}}{\bar{\omega}}$ and $\frac{c}{2\sqrt{k\delta M}}$, the former being the ratio between the angular frequency of the equivalent 1-DOF mass-spring system and the angular velocity of the asteroid while the latter is the damping ratio, again referred to the same equivalent 1-DOF system. For this specific plot $\frac{\sqrt{k/\delta M}}{\bar{\omega}} = 3 \times 10^3$, $\frac{c}{2\sqrt{k\delta M}} = 0.5$ and $n = 10$, $\omega = 0.8$, $\lambda = 0.7$. In the case of the n-DOF system, the velocity of a PM is tracked from the surface until its release and is represented by a blue line. Conversely, $\dot{\chi}$ for the rigid chain model is represented by a red line. Figure 5a compares the behaviour of the two models assuming that the chain is initially at rest for both models. Figure 5b shows the behaviour at steady state. It is apparent from these plots that the velocity in the non-rigid chain model oscillates around the average value provided by the rigid-chain model. Moreover, at steady state, the PM is released with velocity $\dot{\chi} = v_l$ (dashed black line), as predicted by Eq. (37). The results are insensitive to the variation of the stiffness and damping ratio.

2.3 Energy

The kinetic and potential energy of the asteroid and chain at each step are given by:

$$K_j = \frac{1}{2}\left(I_{A,j} + I_{C,j}\right)\bar{\omega}_j^2 + \frac{1}{2}b_j\delta M(\dot{\chi}_j\bar{\omega}_j R)^2 \quad j = 1,\ldots,4 \tag{42a}$$

$$U_j = -\frac{3}{5}G\frac{M_j^2}{R_j} - \sum_{i=1}^{b_j} G\frac{M\delta M}{R_i + \bar{x}_i} \quad j = 1,\ldots,4 \tag{42b}$$

where the summation indexes b_j are the same as in Eqs. (19). The first term in K_j is due to the rotational kinetic energy of the asteroid and chain, while the second term is due to the velocity of the chain in the radial direction. The first term of the potential U_j represents the self gravitational potential of the asteroid, while the second term is the potential of the chain (note that, as the PMs are considered point-like masses, their self potential is neglected).

By substituting Eqs.(18), (19), (21), (23) and (33) into Eqs. (42) it can be verified that $K_1 + U_1 = K_2 + U_2$, i.e., mechanical energy between steps 1 and 2 is conserved at every iteration. Conversely, it can be shown that

$$(K_3 - K_2) + (U_3 - U_2) = E_A + E_{\delta M} \tag{43}$$

where

$$E_A = -\frac{1}{6}\delta M R^2\bar{\omega}_1^2, \tag{44}$$

$$E_{\delta M} = -\frac{1}{2}\delta M\left(R^2\bar{\omega}_3^2(1+\lambda)^2 + (\dot{\chi}_3\bar{\omega}_3 R)^2\right) + G\frac{M\delta M}{R}\frac{1}{1+\lambda}. \tag{45}$$

E_A is the change in kinetic energy due to material rearrangement in the asteroid as each PM is formed (step 3 in Fig. 4): material in the vicinity of the rotation axis (with low moment of inertia) is moved towards the equator (by means of ideal conservative forces), thus decreasing the kinetic energy of the system while conserving the total angular momentum. Conversely, $E_{\delta M}$ is the mechanical energy of the top mass of the chain when released, which is then lost from the system asteroid and chain.

The parameter $E_{\delta M}$ can be normalized by dividing both sides of Eq. (45) by $\delta M(\mu/R)$:

$$\mathcal{E} = \frac{E_{\delta M}}{\delta M(\mu/R)} = \frac{1}{2}\omega^2\left[(1+\lambda)^2 + \dot{\chi}_3^2\right] - \frac{1}{1+\lambda}. \tag{46}$$

In the case of a siphon operating at steady state, with the assumption of $n \to \infty$, $\dot{\chi}_3$ can be replaced by v_l^*. Upon using this substitution Eq. (46) takes the form

$$\mathcal{E} = \frac{1}{4}\omega^2\left[2 + 3\lambda(2+\lambda)\right] - \frac{1}{2}\frac{2+\lambda}{1+\lambda} \tag{47}$$

and becomes a function of ω and λ only. The sign of $\mathcal{E}$ gives immediate information about the motion of the PMs upon release: if $\mathcal{E} < 0$ the motion is bound, whereas for $\mathcal{E} \geq 0$ material is ejected to escape. Note that, if $\mathcal{E} \geq 0$, the normalized energy is linked to the hyperbolic escape speed v_∞ of the released PMs through

$$\frac{v_\infty}{v_{\text{esc}}} = \sqrt{\mathcal{E}} \tag{48}$$

where v_{esc} is the escape velocity at the surface of the asteroid.

Eventually, by substituting Eqs.(18), (21), (23) and (35) into Eqs. (42) it can be shown that mechanical energy is conserved between steps 3 and 4.

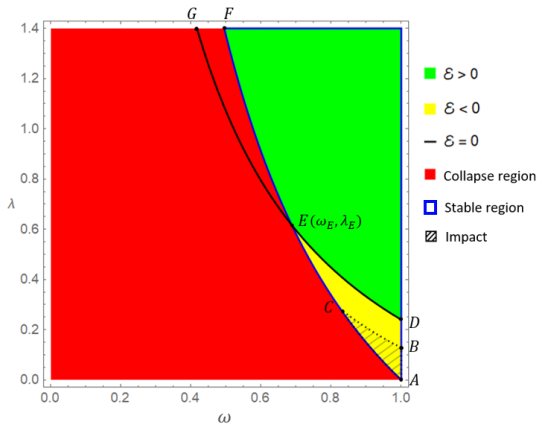

Figure 6: Regions of allowed and forbidden motion as a function of the asteroid normalized angular velocity ω and the normalized chain length λ.

3 Siphon operation

Two conditions must be satisfied to guarantee proper operation of the orbital siphon: *(a)* there must be an overall centripetal-induced pull on the chain of masses and *(b)* if a PM is inserted into an orbit around the asteroid ($\mathcal{E} < 0$) then it must not impact the asteroid later in its motion. Assuming that n is large, condition *(a)* is satisfied if

$$f^* > 0, \tag{49}$$

where f^* is given by Eq. (16). If the first condition *(a)* is satisfied, then material will be inserted either into bound motion around the asteroid or into an escape trajectory, depending on the sign of the normalized energy $\mathcal{E}$, as given by Eq. (47). It can be easily shown that, when $\mathcal{E} < 0$, condition *(b)* is verified if (see Appendix 6.1)

$$\frac{r_p}{R} = -\frac{1}{2\mathcal{E}}\sqrt{1 + 2\mathcal{E}\omega^2(1+\lambda)^4} > 1, \tag{50}$$

where r_p represents the periapsis altitude of the the orbit. It is also assumed that, if material is released into orbit, it is collected by an orbiting-platform before performing one period of rotation around the asteroid, to avoid a collision with the chain. Then, Eqs. (49), (50) and (47) comprehensively describe the behaviour of the orbital siphon as a function of ω and λ (Eq. (49) also depends on the number n of PMs but this is irrelevant when only the sign of f^* is considered). These three conditions partition the ω-λ plane into regions of allowed and forbidden motion, as represented in Fig. 6. The range of λ along the vertical axis has been limited between $\lambda = 0$ and $\lambda = 1.4$ as relevant information about the behaviour of the system is contained within this region. However, in principle, there is not any upper bound on this parameter.

Any configuration falling within the red region (*collapse region*) is associated with a collapsing chain, i.e., a chain with length smaller than its equilibrium length. Complementary to the collapse region is the region with the blue boundary (*stable region*) and it is associated with chains longer than their equilibrium length. The separatrix between the two regions is the curve AF (*equilibrium curve*): if $\lambda \in$ AF then $\lambda = \lambda_{eq}$.

The stable region is then partitioned into two sections. The green region encompasses all configurations releasing PM onto hyperbolic orbits ($\mathcal{E} > 0$). Conversely, material is released into bound motion around the asteroid ($\mathcal{E} < 0$) for a chain within the yellow region. The boundary between these two regions is represented by the

curve ED, which is associated with parabolic motion $\mathcal{E} = 0$. Note that this curve partially intersects the collapse region (curve EG): therefore, for $\omega < \omega_E$ material can be released exclusively into hyperbolic orbits. PMs can be placed into bound motion around the asteroid when the body rotates with $\omega \in [\omega_E, 1]$ (yellow region). The coordinates of the point E can be found at the intersection of two curves $\mathcal{E} = 0$ and $f^* = 0$:

$$\omega_E = \sqrt{2\left(\sqrt{5} - 2\right)} \approx 0.687, \tag{51}$$

$$\lambda_E = \frac{1}{2}\left(\sqrt{9 + 4\sqrt{5}} - 3\right) \approx 0.618. \tag{52}$$

A chain working at point E would release material at escape velocity and, at the same time, be in its equilibrium configuration.

The condition for impact avoidance (Eq. (50)) further restricts the domain of allowed configurations. Any configuration within the impact region (represented with black diagonal lines) identifies a siphon releasing material into bound motion that will eventually impact the asteroid ($r_P/R < 1$). Therefore, the domain of the bound motion region is actually reduced to the region $CBDE$. Thus, the impact region sets a lower bound for the chain length which cannot be less than λ_B (see Table 1 for a summary of the relevant coordinates of Fig. 6).

It can be shown that the region $CBDE$ represents approximately 28% of the bound motion region. Therefore, almost one third of the possible configurations allowed for bound motion must be excluded due to the constraint of impact avoidance. Note that the semi-major axis of the orbit of the released material will increase while the asteroid loses mass [21]. Hence, material released in the $CBDE$ region will remain bound without impacting the asteroid.

Given the above constraints, two possible strategies can be envisaged for siphon operation within the allowed region, i.e., a constant-length chain or a variable-length chain. In both cases, the total amount of extractable mass as a function of the initial angular velocity ω_0 can be found by rearranging Eq. (27) as

$$\frac{1}{5\left(\frac{1}{6} + \lambda + \frac{1}{2}\lambda^2\right)}\frac{\delta\omega}{\omega} = \frac{\delta M}{M} \tag{53}$$

and integrating from ω_0 to $\omega < \omega_0$ and from M_0 to M, which yields

$$\xi_m = \frac{M_0 - M}{M_0} = 1 - e^I \tag{54}$$

with

$$I = \int_{\omega_0}^{\omega} \frac{1}{5\omega'\left(\frac{1}{6} + \lambda + \frac{1}{2}\lambda^2\right)} d\omega' \tag{55}$$

The parameter ξ_m is defined as the *extracted mass ratio*. Ideally, a complete disassembly of the asteroid corresponds to $\xi_m = 1$ and, by analysis of Eq. (54), this requires $I \to -\infty$.

It is possible to find an upper bound for ξ_m when the orbital siphon is releasing material with $\mathcal{E} \geq 0$, using simple energy balance considerations. In fact, for an asteroid spinning at $\omega = 1$, its rotational kinetic energy $K = \frac{1}{2}\left(\frac{2}{5}MR^2\right)(GM/R) = \frac{1}{5}GM^2/R$ is exactly one third of its gravitational binding energy $U = \frac{3}{5}GM^2/R^3$. Assuming that this kinetic energy is entirely used to remove subsequent layers of the asteroid to escape, material can be extracted from the asteroid until the radius $r < R$ is reached, such that:

$$\int_r^R -G\frac{M\delta M}{R} = -\frac{1}{5}G\frac{M^2}{R^3}. \tag{56}$$

Table 1: Coordinates of relevant points in Figs. 6 and 7.

	A	B	C	D	E	H	I	L	M
ω	1	1	0.827	1	0.687	1	0.834	0.768	0.896
λ	0	0.128	0.281	0.240	0.618	0.405	0.405	0.405	0.293

By solving Eq. (56), $r = \sqrt[5]{2/3}R$ which corresponds to

$$\xi_m = 1 - (2/3)^{3/5} \approx 21.5\%. \tag{57}$$

Although the siphon can work at different energy levels, Eq. (57) represents a useful indicator of the maximum theoretical quantity of material which can be released to escape.

In the following sections, the extracted mass ratio is studied for different scenarios: $\lambda = const$ (Sect. 3.1), $\mathcal{E}/(\mu/R) = const$ (Sect. 3.2.3.2.1) and $f^* = const$ (Sect. 3.2.3.2.2). The symbol $\xi_m^{\max}$ is used to indicate the maximum ξ_m when ω is on the curve BCF in Fig. 6.

Undoubtedly, a constant-length chain represents the best choice when considering practical implementation (for example, through conveyor systems [22]). However, as shown in the next section, the best performance in terms of extracted mass is obtained for siphons with variable-length chains (within the simplifying assumptions underpinning this model). Then, the optimal choice will be a trade-off between maximizing the extracted mass or increasing the complexity of the system.

3.1 Constant-length siphon

If the non-dimensional chain length λ is constant during the extraction sequence (*iso-length* extraction), the integral I from Eq. (55) can be trivially solved analytically and the extracted mass ratio becomes

$$\xi_m = 1 - \left(\frac{\omega}{\omega_0}\right)^{1/\gamma} \tag{58}$$

with $\gamma = 5(1/6 + \lambda + \lambda^2/2)$. For a given λ, Eq. (58) indicates the amount of extracted mass when the asteroid has decreased its angular velocity from ω_0 to ω. It has been noted from Fig. 6 that the final angular velocity ω cannot be arbitrarily small: when the curve BCF in Fig. 6 is reached the siphon can no longer work (unless the chain length is allowed to increase, but this case is studied in the next section). Solving Eq. (58) for ω, substituting into Eqs. (6) (if $\lambda \geq \lambda_C$) and (50) (if $\lambda < \lambda_C$) and solving for $f^* = 0$ and $r_p/r = 1$ respectively yields:

$$\begin{aligned} &\xi_m^{\max} = 1 - \left[\frac{1}{\omega_0^2}\frac{1}{(1+\lambda)(1+\lambda/2)}\right]^{\frac{1}{2\gamma}}, && \text{if} \quad \lambda \geq \lambda_C \\ &1 + \tfrac{1}{2}\mathcal{E}^{-1}\left[1 + 2\mathcal{E}\omega_0^2(1-\xi_m^{\max})^{2\gamma}(1+\lambda)^4\right]^{1/2} = 0, && \text{if} \quad \lambda < \lambda_C \end{aligned} \tag{59}$$

Figure 7 shows a contour of $\xi_m^{\max}$ as a function of ω_0 and λ. The maximum extractable mass ratio is approximately 7.7% and corresponds to $\lambda = \lambda_H \approx 0.405$. With $\lambda_D < \lambda_H < \lambda_E$ material is ejected with $\mathcal{E} \geq 0$ for $\omega_0 \in [\omega_I, 1]$ and into bound motion for $\omega_0 \in [\omega_L, \omega_I]$. The red dashed line indicates the optimal λ which maximizes ξ_m as a function of ω_0. Note that for $\omega_0 < 0.82$ the optimal chain length must be larger than the radius of the asteroid.

To perform the entire extraction into bound orbits, ω_0 must be within ω_M and 1. In this case, the optimal chain length varies between λ_B and λ_D with extracted mass ratios up to 5%.

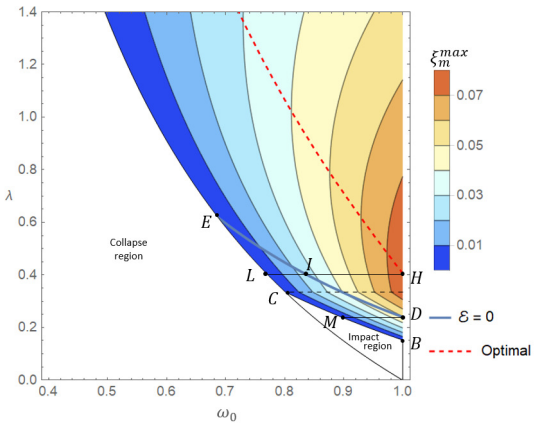

Figure 7: Contour of the maximum extracted mass ratio $\xi_m^{\max}$ as a function of the initial normalized angular velocity ω_0 and the normalized chain length λ for a constant-length siphon. (Eq. (59)).

3.2 Variable-length siphon

In this section the effects of a chain with variable length are investigated. In theory, λ can be changed following any path with decreasing ω in the allowed region of Fig. 6. In particular, in Sect. 3.2.1 λ is varied by keeping the release energy $\mathcal{E}$ constant (*iso-energy*), while in Sect. 3.2.2 by keeping the force f^* constant (*iso-force*) and equal to zero (i.e., the siphon is working along the equilibrium curve).

The choice of these paths is motivated by the following reasons. By analysis of the iso-energy curves it is possible to understand the maximum ξ_m with the minimum energy necessary to escape ($\mathcal{E} = 0$) and compare it with other energy regimes. Conversely, the iso-force curve at equilibrium offers insight into the maximum amount of extractable material by keeping the chain length at the minimum allowed. In the latter case, then, the variation of angular velocity at each step of the sequence described in Sect. 3 is minimized (Eq. (24)).

3.2.1 Constant non-dimensional specific energy

In this scenario λ and ω vary according to Eq. (47) with $\mathcal{E}$= *const*. The domain of possible iso-energy curves is restricted between $\mathcal{E} \approx -0.219$ and $\mathcal{E} = 1$ (Fig. 8). When $\mathcal{E} > 1$ the iso-energy curves never cross the equilibrium curve, thus leading to a degenerate case of an infinitely increasing chain (for $\mathcal{E} = 1$, the two curves ideally intersect at $\omega = 0$, where $\lambda \to \infty$). Conversely, when $\mathcal{E} < -0.219$ the iso-energy curve would cross the impact region. The lower iso-energy curve passes through the point C (the iso-energy curve through B has lower energy and would therefore cross the impact region).

The extracted mass ratio can be found solving Eq. (47) for λ and then substituting into Eq. (55). Equation (55) is then integrated from ω_0 to $\omega < \omega_0$ where the iso-energy curve crosses the equilibrium curve. Figure 9a shows a plot of $\xi_m^{\max}$ as a function of $\mathcal{E}$ within the energy domain for some values of the initial angular velocity ω_0. The maximum $\xi_m^{\max}$ is obtained for $\omega_0 = 1$, $\mathcal{E} = 0.224$ and is approximately 11%. For any other initial velocity $\omega_0 < 1$ the energy of the optimal iso-energy curve is larger and $\xi_m^{\max}$ decreases. For $\omega_0 = 0.7$ the maximum extractable mass is less than half the maximum found for $\omega_0 = 1$. In any case, optimal iso-energy extraction requires $\mathcal{E} > 0$, therefore material is released on a hyperbolic trajectory with a hyperbolic

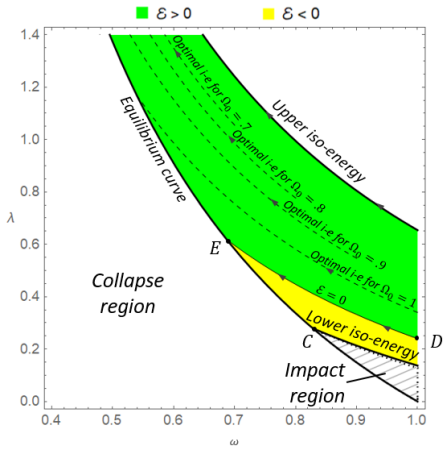

Figure 8: Domain for the iso-energy curves in the ω-λ plane. The dashed lines represents the optimal iso-energy obtained for four different ω_0.

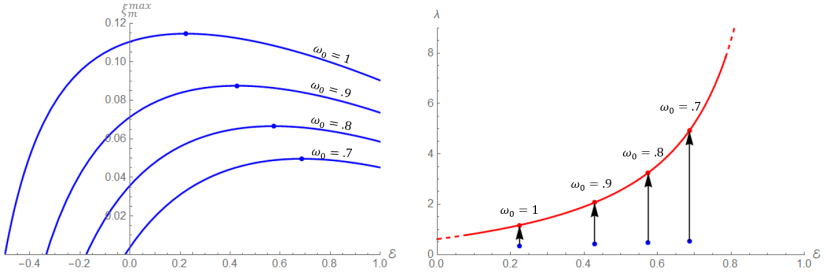

(a) (b)

Figure 9: (a) Extractable mass as function of $\mathcal{E}$ for different ω_0. (b) Variation of λ on four optimal iso-energy curves corresponding to different ω_0.

excess speed which is at least half the escape velocity at the surface (Eq. (48)) [2]. It is also apparent from Fig. 8 that ω decreases significantly from the beginning to the end of the iso-energy curve.

For a given energy, the normalized length of the chain varies between a minimum (when $\xi_m = 0$) and a maximum (when $\xi_m = \xi_m^{\max}$), as represented in Fig. 9b for different ω_0. For $\omega_0 = 1$, the final chain length is comparable with the radius of the asteroid, however for lower ω_0 the final length becomes much larger (approximately five times the radius of the asteroid for $\omega_0 = 0.7$). On the contrary for negative energies, $\lambda < 1$.

For a given ω_0, the iso-energy with $\mathcal{E} = 0$ provides extractable ratios comparable with the optimal case only for ω_0 close to 1 (Fig. 9a). Eventually, when $\omega < \omega_E$ extraction in bound orbits is not allowed.

3.2.2 Equilibrium length

In this section the case with $f^* = 0$ is analysed, which is the best-case scenario to maximize the amount of extractable mass. In fact, it is apparent from analysis of Eq. (54) that ξ_m is maximum when I is minimum (note that $I < 0$). Given ω_0 and ω, the integral I is minimized when λ is minimum, i.e., when $f = 0$. In this case, although the siphon is initially in equilibrium for $\chi = 0$, an infinitesimal perturbation can initialize the siphon effect, since the equilibrium is unstable. Again, it is assumed that $n \to \infty$: in this case λ varies along the equilibrium curve in Fig. 6. Note that, the section AC of the equilibrium curve is also the boundary of the impact region: for a chain operating in such conditions, material would be released into an orbit with periapsis equal to the radius of the asteroid. For this reason, AC is excluded from the domain of this analysis, meaning that $\omega_0 \leq \omega_C$. However, if $\omega_0 \in [\omega_C, 1]$, the point C can be approached through the lower iso-energy curve (Fig. 8).

The extracted mass ratio in this scenario is evaluated by substituting Eq. (17) into Eq. (54), where the integral I is evaluated from $\omega_0 \leq \omega_C$ to $\omega < \omega_0$. The maximum ξ_m is evidently found when the initial angular velocity is the maximum allowed in the domain just defined, i.e., $\omega_0 = \omega_C$.

The blue curve in Fig. 10 represents the evolution of $\xi_m^{\max}$ as a function of λ, assuming that $\omega_0 = \omega_C$ (and, accordingly, $\lambda = \lambda_C$). The theoretical maximum extractable mass is reached when the chain is infinitely long and is approximately 12% of the asteroid initial mass. However, when the chain has reached twice the radius of the asteroid, the extracted mass ratio has already reached 85% of the theoretical maximum. The process releases PMs into bound orbits between $\lambda_C < \lambda < \lambda_E$ and into a hyperbolic trajectory for $\lambda > \lambda_E$. It is apparent from Fig. 10 that almost half of the extractable material is released into a bound orbit. Clearly, if $\omega_0 < \omega_C$ then $\lambda_0 > \lambda_C$ and ξ_m will be lower than 12%. For comparison, the red curve on Fig. 10 shows the evolution of ξ_m from $\omega_0 = \omega_E$.

It is interesting to evaluate $\xi_m^{\max}$ taking into account the section AC of the equilibrium curve, as a measure of the maximum disassembly capabilities of the orbital siphon. In this case, a body rotating with $\omega_0 = 1$ is considered and the equilibrium curve is followed from point A (see orange curve in Fig. 10). Then, Eq. (54) has an analytical solution for this scenario:

$$\xi_m^{\mathrm{MAX}} = \lim_{\omega \to 0^+} \xi_m^{\max} = 1 - \exp\left(\log 48 + \sqrt{6}\log(5 - 2\sqrt{6})\right) \approx 0.23. \tag{60}$$

This value is almost twice the maximum extractable mass found for $\omega_0 = \omega_C$. It is apparent from Fig. 10 that more than half of this material would be extracted inside

[2] Note that as material is extracted the escape velocity at the surface varies. However the ratio between the hyperbolic excess velocity of the released PM and the escape velocity remains constant, as dictated by Eq. (48)

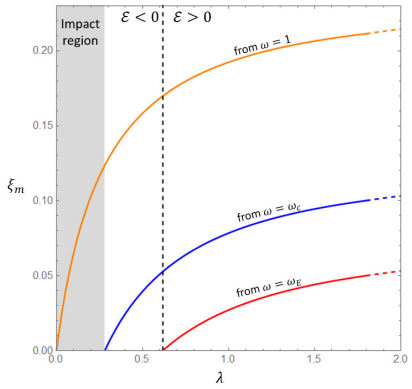

Figure 10: Extractable mass for three iso-force curves (at $\tilde{f} = 0$) as a function of λ. The dashed black line marks the transition between negative and positive release energy $\mathcal{E}$.

the impact region, using chains with maximum length up to $\lambda_C \approx 0.281$. Hence, the impact avoidance constraint excludes a valuable region which would enable large mass extraction with $\mathcal{E} < 0$. However, it is easy to show that a chain with a braking mechanism at the base, which reduces to zero the radial velocity of a PM at release, would move the impact region inside the collapse region, thus increasing the overall realm of allowed configurations. In this case, not only the orbital siphon works in the range $\omega = 1$ and $\omega = \omega_C$ but also braking may be used in principle to generate power.

Although not directly comparable, it is interesting to observe that ξ_m^{MAX} in Eq. (60) is close to the theoretical 21.5% specified in Eq. (57), found from basic energy balance considerations. In this case, ξ_m is slightly larger as part of the extraction is performed with $\mathcal{E} < 0$, thus releasing material into bound orbit and not to escape. In both cases, however, ξ_m is always below one quarter of the initial mass.

4 Discussion

Table 2 shows the relevant parameters (in dimensional form) obtained in the case of a fixed-length siphon operating at the optimal length (Sect. 3.1) for some candidate asteroids. Asteroid data are taken from the *Asteroid Lightcurve Database* [23] and five asteroids with $R < 1000\,\mathrm{m}$ are chosen and listed in descending order of extractable mass (ΔM). Data are calculated assuming the asteroid is a sphere with uniform density. Density values are chosen depending on the asteroid class, as described in [24]. As expected, these objects are fast rotators, with rotation periods below 3.5 h. For these candidates, optimal chain lengths vary between 671 m and 977 m and the maximum extractable mass is on the order of 10^{11}kg.

The time to raise a PM ($\bar{P}$), the number of released PMs per period (N) and the radial velocity of the chain at release ($\bar{v}_l$) are calculated assuming $n = 25$ and $\omega = \omega_0$ (In general, these parameters will change as more mass is separated from the asteroid, following the analysis in Sect. 32.2). The radial velocity of the chain for all the candidates is below $1\,\mathrm{m\,s^{-1}}$ while the time to raise a single PM is below 100 s.

It is important to note that these values are independent from the mass δM of the PMs. Clearly, by increasing δM (and, in turn, the released mass rate) the Coriolis force acting on the chain would increase, and therefore a larger anchoring force would be required to keep the chain vertical. However, it has been shown in [22] that removing the hypothesis of a tether rigidly fixed at the surface, the resulting in-plane equatorial

Table 2: Relevant chain characteristics for some asteroids assuming optimal iso-length extraction.

Asteroid	Radius [m]	Period [hours]	ω_0	$\bar{L}$ [m]	$\xi_m^{\max}$	ΔM [kg]	$\bar{P}$ [s]	N	$\bar{v}_l$ [m/s]
McAuliffe	995	2.21	0.911	671	0.056	6.27×10^{11}	53.4	149	0.51
Tantalus	940	2.38	0.843	850	0.045	4.19×10^{11}	62.2	138	0.56
1997 UF9	855	2.40	0.837	791	0.044	3.09×10^{11}	62.9	137	0.51
2000 PN9	895	2.53	0.793	977	0.038	3.04×10^{11}	69.1	132	0.58
2001 MK3	980	3.27	0.885	745	0.051	2.63×10^{11}	81.7	144	0.37

oscillations of the system would have negligible amplitude (on the order of milliradians) if a counterweight is connected to the chain and, therefore, the orbital siphon effect would still be stable.

Nonetheless, the issue of keeping the chain vertical could be ignored if a storing/processing spacecraft is connected directly at the end the chain. In this case, not only would the spacecraft act as counterweight, thus naturally reducing the amplitude of the resulting oscillations, but also the problem of collecting the PMs after release would be avoided.

The choice of δM also influences the rate of released material $\dot{m}_{\text{siphon}} = \delta M/(\bar{P})$. In [22] it has been shown that rates up to $20\,\text{kg}\,\text{s}^{-1}$ can be achieved for a candidate asteroid (taking into account constraints on the Coriolis force, anchoring force, tether tensions and oscillations of the system). This value is much larger with respect to the maximum mining rate suggested by [25, 26] between 300 and 1000 kilograms per day. Then, the siphon can operate at the rate driven by the mining rovers and could actually withstand much larger mass flow rates.

When compared to standard propulsion systems, the orbital siphon concept becomes effective for a large amount of mined mass to be lifted from the surface. As an example, assuming the entire extractable mass ΔM of the first asteroid of Table 2 is sent to escape, a propellant mass $m_{\text{prop}} = \Delta M \frac{M_f}{1-M_f} = 1.39 \times 10^8\,\text{kg}$ is required, where the propellant mass fraction is $M_f = 1 - \exp(-v_{\text{esc}}/v_e)$ and v_{esc}, v_e are the escape velocity and effective exhaust velocity respectively (in this case it is assumed $v_e = 4.2\,\text{km}\,\text{s}^{-1}$, as in [25]). Then, the siphon becomes more efficient than the propulsion system when its mass m_{siphon} is less than m_{prop} and, although an estimate of the siphon mass has not been provided here, it is reasonable to assume $m_{\text{siphon}} << m_{\text{prop}}$. We note however that an electromagnetic mass driver could be used to lift payload masses without the need for reaction mass.

It should be emphasized that the energy required to transport material from different part of the asteroid to the siphon has not been considered here. Although this problem requires detailed additional investigation, the energy requirements might be minimized if multiple orbital siphons are envisaged, distributed along the equatorial region of the asteroid.

Eventually, further analysis is required to understand the behaviour of the system in response to non-uniform gravity fields or in the case of non-primary axis rotators. However, the irregularity of the gravitational field would be relevant only in the close vicinity of the asteroid, while the behaviour of the system will be mainly influenced by the centripetal-induced lifting force in the outer region of the chain. Hence, it is reasonable to conclude that irregular gravity fields will change the minimum length of the chain required for the equilibrium, but the overall dynamics will not be dramatically different with respect to what has been outlined in the present work.

5 Conclusion

It has been shown that, considering a spherical rotating asteroid, a vertical chain of masses can be envisaged to overcome the surface gravity of the body and lift material without the need for external work to be done. Under specific conditions, the centripetal-induced force on the uppermost masses can be large enough to pull the lower masses. Thus, by releasing the top mass of the chain and adding a new payload mass at the bottom, an orbital siphon mechanism is initialized, and a stream of masses can be released with a range of energies, which depends on the physical characteristic of the asteroid (its angular velocity and density) and the chain (its length). In particular, material can be released into bound orbits around the asteroid and into parabolic or hyperbolic orbits. However, only fast rotators with an angular velocity larger than approximately 68% of their critical angular velocity can release material into bound motion.

Three strategies of mass extraction have been investigated, involving chains with constant and non-constant length. Optimal chain configurations for these cases have been discussed. In optimal conditions, the maximum extractable mass is within approximately 8 and 12% of the initial mass of the asteroid, where larger values are possible for fast rotators and variable-length chains. However, it has been pointed out that longer chains also increase the complexity of the system when considering practical implementation.

Although, in general, the practical implementations of such concepts are undoubtedly challenging (for a wide variety of problems, including proper anchoring, material selection, optimal design, etc) this paper has shown that the orbital siphon effect could be utilised to extract a valuable quantity of mass from an asteroid by leveraging its rotational energy, without the need for external work to be done, and therefore offers scope for further investigation.

6 Appendix

6.1

Let d be the distance from the surface of the asteroid at which PMs are released. Let $v_\perp$ and v_r be the radial and tangential velocities at release respectively. Then $v_\perp = \bar{\omega}R$ and v_r is given (in its normalized form) from Eq. (38). If material is released into an orbit with eccentricity e and semi-major axis a then:

$$E = -\frac{\mu}{2a} = \frac{v_\perp^2 + v_r^2}{2} - \frac{\mu}{R+d} < 0 \tag{61}$$

where E is the (constant) specific energy of the orbit and a its semi-major axis. At the periapsis r_p:

$$E = \frac{h^2}{2r_p^2} - \frac{\mu}{r_p} \tag{62}$$

where $h = v_p r_p$ is the angular momentum per unit mass of the orbit and v_p is the velocity at the periapsis. Since $r_p = \frac{h^2}{\mu}\frac{1}{1+e}$ [27], Eq. (62) becomes:

$$E = -\frac{1}{2}\frac{\mu^2}{h^2}(1-e^2). \tag{63}$$

The angular momentum per unit mass is also equal to the product $h = v_\perp(R+d)$, hence Eq. (63) can be written as:

$$E = -\frac{1}{2}\frac{\mu^2}{v_\perp^2(R+d)^2}(1-e^2). \tag{64}$$

Moreover, the periapsis r_p of the orbit can be expressed as a function of the semi-major axis and the eccentricity:

$$r_p = a(1 - e). \tag{65}$$

Solving Eq. (61) and (64) for a and e respectively and substituting into Eq. (65) yields, after simplifications:

$$\frac{r_p}{R} = -\frac{1}{2\mathcal{E}}\sqrt{1 + 2\mathcal{E}\omega^2(1+\lambda)^4} \tag{66}$$

where $\mathcal{E}$ is the non-dimensional specific energy ($\mathcal{E} = E/(\mu/R)$). Then, if $r_p/R \leq 1$ material will impact the asteroid.

References

[1] Ross SD. 2001 Near-earth asteroid mining. *Caltech Internal Report.*

[2] Sanchez JP, McInnes CR. 2012 Assessment on the feasibility of future shepherding of asteroid resources. *Acta Astronautica* **73**, 49–66.

[3] Lewis JS. 1997 Resources of the Asteroids. *Journal of the British Interplanetary Society* **50**, 51–58.

[4] McInnes CR. 2017 Harvesting Near Earth Asteroid Resources Using Solar Sail Technology. *4th Int. Symp. on Solar Sailing (ISSS 2017).*

[5] Pearson J. 1997 Konstantin Tsiolkovski and the origin of the space elevator. In *48th IAF, International Astronautical Congress, Turin, Italy* vol. 10 pp. 6–10.

[6] Tsiolkovsky K. 2004 *Dreams of Earth and Sky.* The Minerva Group, Inc.

[7] Artsutanov Y. 1960 V kosmos na elektrovoze. *Komsomolskaya Pravda* **31**, 946–947.

[8] Pearson J. 1975 The orbital tower: A spacecraft launcher using the Earth's rotational energy. *Acta Astronautica* **2**, 785–799.

[9] Clarke AC. 1981 Space Elevator:" Thought Experiment," or Key to the Universe.. *Adv. Earth oreiented applic. space tech* **1**, 39–48.

[10] Edwards BC. 2000 Design and Deployment of a space elevator. *Acta Astronautica* **47**, 735–744.

[11] Pugno NM. 2006 On the strength of the carbon nanotube-based space elevator cable: from nanomechanics to megamechanics. *Journal of Physics: Condensed Matter* **18**, S1971.

[12] Pugno N, Schwarzbart M, Steindl A, Troger H. 2009 On the stability of the track of the space elevator. *Acta Astronautica* **64**, 524–537.

[13] Woo P, Misra AK. 2010 Dynamics of a partial space elevator with multiple climbers. *Acta Astronautica* **67**, 753–763.

[14] Woo P, Misra AK. 2013 Mechanics of very long tethered systems. *Acta Astronautica* **87**, 153–162.

[15] Cohen S, Misra AK. 2015 Static deformation of space elevator tether due to climber. *Acta Astronautica* **111**, 317–322.

[16] Williams P. 2009 Dynamic multibody modeling for tethered space elevators. *Acta Astronautica* **65**, 399–422.

[17] McInnes CR. 2005 Dynamics of a Particle Moving Along an Orbital Tower. *Journal of Guidance, Control, and Dynamics* **28**, 380–382.

[18] McInnes CR, Davis C. 2005 Novel Payload Dynamics on Space Elevators Systems. *56th International Astronautical Congress.*

[19] Logsdon T. 1998 *Orbital mechanics: theory and applications*. John Wiley & Sons.

[20] Abramowitz M, Stegun IA. 1964 *Handbook of mathematical functions: with formulas, graphs, and mathematical tables* vol. 55. Courier Corporation.

[21] Hadjidemetriou JD. 1966 Analytic solutions of the two-body problem with variable mass. *Icarus* **5**, 34–46.

[22] Viale A, McInnes CR, Ceriotti M. 2018 Disassembly of Near Earth Asteroids by leveraging rotational self energy. *69th International Astronautical Congress, IAC-18-D4.3-18*.

[23] Warner BD, Harris AW, Pravec P. 2009 The asteroid lightcurve database. *Icarus* **202**, 134–146.

[24] Chesley SR, Chodas PW, Milani A, Valsecchi GB, Yeomans DK. 2002 Quantifying the risk posed by potential Earth impacts. *Icarus* **159**, 423–432.

[25] Dorrington S, Olsen J. 2017 Mining Requirements for Asteroid ore Extraction. *68th International Astronautical Congress IAC-17,D4,5,2*.

[26] Sonter MJ. 1997 The technical and economic feasibility of mining the near-earth asteroids. *Acta Astronautica* **41**, 637–647.

[27] Vallado DA. 2001 *Fundamentals of astrodynamics and applications* vol. 12. Springer Science & Business Media.